Comparing Sulfidation Kinetics of Silver Nanoparticles in Simulated Media using Direct and Indirect Measurement Methods

Journal:	*Nanoscale*
Manuscript ID	NR-ART-08-2018-006668.R1
Article Type:	Paper
Date Submitted by the Author:	05-Nov-2018
Complete List of Authors:	Liu, Jingyu; National Institute of Standards and Technology, Zhang, Fan; NIST, Materials Measurement Science Division Allen, Andrew; NIST, Material Measurement Laboratory Johnston-Peck, Aaron; National Institute of Standards and Technology, Pettibone, John; National Institute of Standards and Technology, Material Measurement Laboratory

Comparing Sulfidation Kinetics of Silver Nanoparticles in Simulated Media using Direct and Indirect Measurement Methods

*Jingyu Liu, Fan Zhang, Andrew Allen, Aaron C. Johnston-Peck and John M. Pettibone**

**john.pettibone@nist.gov*

Abstract

Reported reaction kinetics of metal nanoparticles in natural and engineered systems commonly have used proxy measurements to infer chemical transformations, but extension of these methods to complex media has proven difficult. Here, we compare the sulfidation rate of AgNPs using two ion selective electrode (ISE)-based methods, which rely on either i) direct measurement of free sulfide, or ii) monitor the free Ag^+ available in solution over time in the presence of sulfide species. Most experiments were carried out in moderately hard reconstituted water at pH 7 containing fulvic acid or humic acid, which represented a broad set of known interferences in ISE. Distinct differences in the measured rates were observed between the two proxy-based methods and details of the divergent results are discussed. The two ISE based methods were then compared to direct monitoring of AgNP chemical conversion to Ag_2S using synchrotron-based *in situ* X-ray diffraction (XRD). Using XRD, distinct rates from either ISE-based technique were observed, which demonstrated that ISE measurements alone are inadequate to discriminate both the rate and extent of AgNP sulfidation. XRD rate data elucidated previously unidentified reaction regimes that were associated with AgNP coating (PVP and citrate acid) and NOM components, which provided new mechanistic insight into metallic NP processing. In general, the extent of Ag_2S formation was inversely proportional to surface coverage of the initial AgNP. Overall, methods to determine reaction kinetics of nanomaterials in increasingly complex media and heterogeneous size distributions to improve NP-based design and performance will require similar approaches.

Introduction

The pathways for nanomaterial transformations are driven by the competing reactions with different rates in the system. Isolating and monitoring the relative rates of reactions facilitates improved design for performance and sustainability. The chemical transformations of metallic nanoparticles in aqueous suspensions, either dispersed or supported on a substrate or within a matrix, commonly undergo corrosion pathways (e.g., oxidation, sulfidation).[1, 2] The resulting corrosion products are often semiconductors, and these metal-semiconductor hybrid nanoparticle-based systems are of broad interest for electronic, optical and photocatalysis applications. Understanding of the corrosion process is also of paramount importance for predicting the lifetimes and fate of metallic nanoparticles in environmental systems.

For metallic nanoparticles, the competing reactions can be difficult to deconvolute and even more challenging to monitor in applied and natural systems. Silver nanoparticles represent an important commercial class of metallic nanoparticles that undergo complex reaction pathways during transformations, i.e., multiple reactions occurring simultaneously. To begin to identify these reaction pathways, growth and transformations of industrially important nanoparticle systems using *in situ* X-ray scattering methods have been reported.[3, 4] The ability to directly monitor specific reactions and elucidate mechanistic details of the transforming NPs provide a route to better understanding the complex transformation pathways that metallic nanoparticles undergo in systems of interest. However, no reports employing these techniques have been reported to systematically investigate the mechanistic contributions from different molecular and structural contributions combined with thorough surface characterization, which are all required to predictively improve nanomaterial design.

Sulfidation represents a prominent transformation pathway for AgNPs in natural and biological systems,[5] and thus, a body of literature exists that has examined different aspects of the transformation network. The seminal work by Liu et al.,[6] examined the mechanism of AgNP sulfidation at relatively high and low concentrations of sulfide and reported the mechanistic transformations with relative rates of the competing oxidation and sulfidation reactions. To determine sulfidation kinetics in the two regimes, ion selective electrodes (ISE) were used to monitor sulfide ion depletion as a proxy for AgNP sulfidation in the presence of low concentrations of known interfering species, e.g., natural organic matter. The majority of studies that have examined AgNP sulfidation rely on proxy measurements to determine the mechanism and measure the associated transformation rates using ISE, dissolved metal ion determination, or other colorimetric techniques (e.g., methylene blue standard method) that do not directly measure the conversion of the AgNP, which have been summarized elsewhere.[7-9] The ISE[10] and colorimetric[11] based methods are cost-efficient and have been extensively used to monitor AgNP sulfidation process.[12-15] However, without comparison to measurement methods that directly monitor the chemical changes of the metallic NPs, which has not been presented in the literature to date, the relative reaction rates for specific transformation pathways cannot be determined. Thus, the mechanisms derived using the aforementioned methods cannot be validated, which ultimately limit their value for predictive modeling.

In the current study we have examined the sulfidation of uniformly sized AgNPs using commonly employed ISE methods and a direct synchrotron-based approach, *in situ* X-ray diffraction. Here the capacity of each method to temporally monitor chemical changes to the AgNP core, i.e., changes from Ag^0 to Ag_2S, and distinguish reaction regimes that could be differentiated by changes in observed reaction rates was examined. Transmission electron microscopy (TEM) was used to corroborate the ensemble measurement

findings. The role of natural organic matter (NOM) components, ligand coating and pH are investigated to demonstrate the information that can be gleaned from the commonly used methods to more accurately assess dynamic systems. Although the current system has simulated natural organic components and macromolecules in the ligand shell, the methods used are also relevant for improving nanomaterial design in applied systems using small molecules to affect their interfacial properties and overall performance.

Materials and Methods

The AgNPs used in this study were research grade NIST RM 8017, a lyophilized PVP (molar mass approximately 40 kDa) coated AgNPs with nominal diameter of 75 nm.[16] Each vial of RM 8017 composed of 2.1 mg AgNPs and 20 mg PVP was reconstituted into suspension by adding 2 mL of deionized water. The obtained AgNP suspension (1 mg Ag mL^{-1}) was purified with one water wash cycle by ultrafiltration (Amicon Ultra-4, nominal molecular weight limit of 100 kDa, EMD Millipore, MA)[1] to remove unbound PVP. Subsequently, the purified AgNPs were concentrated to 4.3 mg mL^{-1} and stored at 4 °C in the dark for future use. The citrate coated AgNPs were nominally 70 nm (Biopure, Nanocomposix, CA). The $Na_2S{\cdot}9H_2O$ (≥ 99.99% trace metal basis), $AgNO_3$ (≥ 99%) were purchased from Sigma-Aldrich. The Suwannee River Fulvic Acid Standard II (FA) and Humic Acid Standard II (HA) were acquired from International Humic Substance Society. The moderately hard reconstituted water (MHRW) was prepared according to an EPA protocol.[17] Sulfide antioxidant buffer (SAOB,) and silver ionic strength adjuster (ISA) used for ISE measurements were purchased from Thermo Scientific.

*Sulfidation kinetics monitored by ISE***.**

AgNP sulfidation was tracked by time-resolved measurements of sulfide depletion using a silver/sulfide ISE (9616BNWP Sure-Flow® Solid State Combination ISE, Thermo Scientific). Two approaches, namely i) sulfide direct calibration and ii) analyte subtraction, were applied to quantify the reduced sulfide. Both methods are independent of the molar S to Ag ratio for the concentration range of analytes examined. The analytes for the measurements are free sulfides present in solution that are used as a proxy to infer reaction extent. The direct calibration approach uses linear calibration curve of sulfide (limit of detection 0.2 mg L^{-1}) constructed daily from fresh Na_2S standards. A sulfide antioxidant buffer (SAOB) solution was added into standards and samples to prevent oxidation. On the other hand, the analyte subtraction method relies on stoichiometric formation of Ag_2S, where the ISE quantifies change of Ag^+ concentration upon reacting spiked $AgNO_3$ with sulfide sample. At desired time points, known amount of $AgNO_3$ (in excess to sulfide) was spiked into samples to quench the sulfidation reaction. Subsequently, the sulfide concentration is computed based on Ag^+ consumption. Principle of these two methods are explained in detail in the electronic supplementary information (ESI). Because Ag^+ binds strongly with sulfur(II-) in inorganic and organic compounds,[24] this approach is expected to detect both inorganic ($H_{2-n}S^{n-2}$) and organic sulfur compounds that are available for sulfidation. An ionic strength adjusting (ISA) solution was added to maintain constant background ionic strength for standards and samples. The possible interference from NOM, AgNPs, and MHRW to ISE response of Ag^+ was examined in control experiments. In all cases, the relative differences between the measured Ag^+ to spiked Ag^+ were ≤ 6 %, demonstrating that this approach is feasible in conditions used in this study. The limit of detection for the analyte subtraction method depends

[1] The identification of any commercial product or trade name does not imply endorsement or recommendation by the National Institute of Standards and Technology.

on whether the added sulfide can result in a detectable change in ISE response for Ag^+. In our experiments, a limit of detection of ~ 1 mg L^{-1} sulfide was achieved.

The sulfidation experiments were conducted in MHRW at sulfide/AgNP molar ratio, [S]/[Ag], of 0.7 and FA/AgNP mass ratio (m_{FA}/m_{Ag}) of 0 and 5. Prior to experiments, FA stocks of 50 mg mL^{-1} were prepared by adding water into lyophilized FA powder. This FA solution was rotated overnight to promote dissolution. Subsequently, the pH of FA stocks was adjusted to ≈ 7 with NaOH. Two AgNP concentration levels were evaluated: (1000 - 1400) mg L^{-1} and 150 mg L^{-1}, with final sample volume of 1 mL and 7 mL, respectively. The high dose experiments were used to directly compare with synchrotron-based X-ray scattering measurements of AgNP cores. Samples were prepared in glass vials protected from light. In a typical experiment, desired amount of purified AgNP stock was added into pH adjusted solutions (with or without FA) and manually mixed by shaking for 10 s. Subsequently, a freshly prepared Na_2S solution was added last to minimize unwanted reactions between sulfide and FA.[18, 19] The Na_2S solution was used within 10 min to minimize oxidation, and the initial recovery of reduced sulfide was in the range of 82 % - 94 % by ISE analysis. In selected experiments, AgNPs were incubated with FA for > 2 h to allow surface adsorption of FA prior to addition of Na_2S. In addition, control samples of Na_2S and Na_2S/FA in MHRW under the same conditions were carefully examined. The vials were covered with perforated parafilm to ensure air saturation. Samples were agitated on a vortex mixer at 300 rpm, and aliquots were taken for sulfide measurements at chosen time points. Specifically in ISE analysis via the analyte subtraction approach, 2.5 mL of (50 – 80) mg L^{-1} Ag^+ (as in $AgNO_3$) was added into 0.05 ml aliquot of high dose samples, while 2.5 mL of (25 – 50) mg L^{-1} Ag^+ was added into 0.25 ml aliquot of low dose samples. The uncertainty reported in the measurements represents 1σ for at least triplicate measurements and the reproducibility was examined over multiple samples ($n > 2$).

Sulfidation kinetics monitored with X-ray diffraction.

Synchrotron USAXS, SAXS and WAXS experiments were performed at the USAXS facility at the Advanced Photon Source (APS), Argonne National Laboratory.[11] The absolutely-calibrated USAXS experiments were conducted with Bonse-Hart optics in the standard 1-D collimated geometry. The SAXS and WAXS experiments were conducted using two standalone Pilatus 2-D area detectors (Model: 100K-S, Dectris, Baden, Switzerland).[12] Data were acquired following a repeated sequence of USAXS, SAXS, and WAXS measurements. Each set of USAXS/SAXS/WAXS measurement took ≈ 5 min. More details about *in situ* synchrotron experiments and data analysis can be found elsewhere.[20]

Results and Discussion

Sulfide depletion kinetics determined by ISE

To evaluate whether sulfide consumption correlates directly with AgNP sulfidation in the current systems, we compared results from both ISE methods at two different Ag concentrations in different simulated media to state-of-the-art *in situ* XRD. First, ISE was used to study sulfidation kinetics of PVP-coated AgNPs reacted with [S]/[Ag] = 0.7±0.02 in MHRW and excess FA ($m_{FA}/m_{Ag} = 5$). Figure 1A shows the time-resolved sulfide measurements by the direct calibration approach. In this approach, the ISE response measures reduced sulfide ($H_{2-n}S^{n-2}$) that is electrochemically active and is freely exchangeable between solution phase and sensing membrane. Upon Na_2S addition into AgNPs/FA suspension (the green triangle trace, condition 1), sulfide decreased abruptly and dropped below the limit of detection within 60

min. Increasing AgNP incubation time with FA to allow adsorption equilibrium prior to sulfidation showed no difference (the blue cross trace, condition 2).

However, Na_2S controls in the absence and presence of FA gave distinct results: while the decrease of sulfide in MHRW was rather moderate (the black square trace, condition 3), Na_2S exposed to FA alone (the red circle trace, condition 4) resulted in measured depletion rates statistically equivalent to AgNP containing systems. The data from condition 1, 2 and 4 were fit with the pseudo first order kinetic law, $-dC_t / dt = k_{obs} \times C_t$ to obtain rate coefficients, k_{obs}, of (0.099 ± 0.008) min^{-1}, (0.090 ± 0.002) min^{-1}, and (0.096 ± 0.002) min^{-1}, respectively, where the uncertainty represents standard error of the fit.[10] All rate data is summarized in Table 1. The difference in k_{obs} is likely within the uncertainty of ISE measurement.[21, 22] Data in sulfide only solutions (condition 3) exhibit a more complex kinetics, showing an induction period (apparent rate closes to nil)[23] followed by first-order oxidation at rate constant of 0.002 ± 0.001 min^{-1}. Clearly, reaction rate of solution-phase sulfide-oxidation by dissolved oxygen alone[23] is significantly slower than sulfide-consumption in the presence of FA. In addition, the near-identical sulfide-depletion rates in condition 1, 2 and 4 strongly indicate a predominant role of FA as free sulfide sink in these systems. It is reasonable to surmise the initial sulfide decay is primarily attributed to interaction between Ag and NOM components. We note that previous studies reported rather minor contributions from NOM components on the sulfidation of AgNPs,[10, 11] where experiments were conducted in low NOM concentrations ($m_{NOM} \leq 20$ mg L^{-1}) and low mass fractions of NOM to AgNPs ($m_{NOM}/m_{Ag} < 1.0$). In this study, we used high relative FA at $m_{FA}/m_{Ag} = 5$ to better represent AgNP exposure in natural environments.

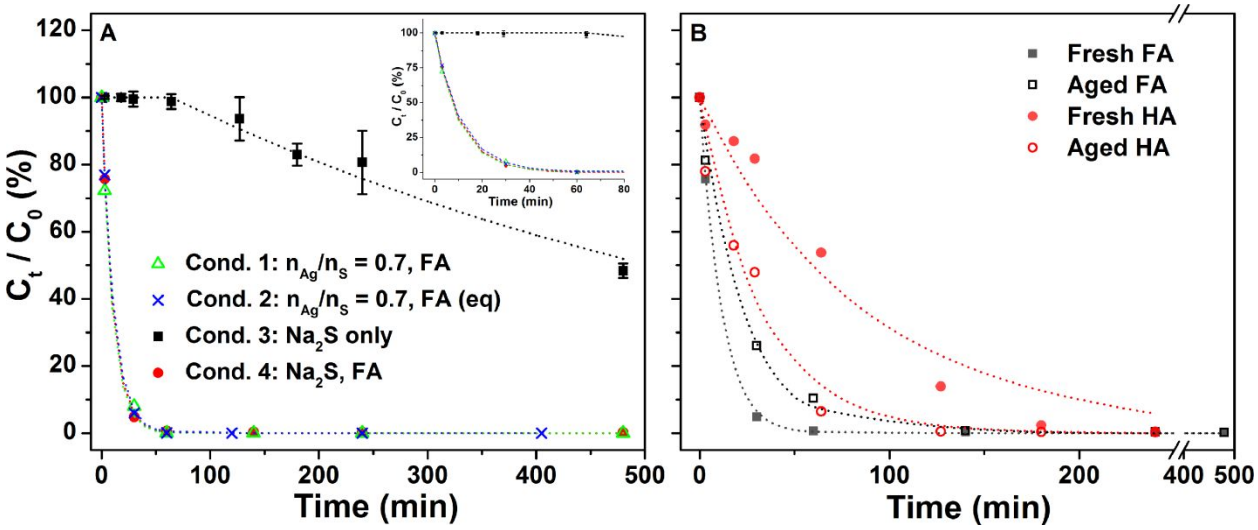

Figure 1. Sulfide depletion kinetics measured by ISE *via* the direct calibration approach. (A) Time-resolved sulfide measurement during AgNPs sulfidation in the presence of FA, showing indistinguishable rates for AgNP samples and Na_2S control in FA systems (Insert shows data ranging from 0 – 80 min). The concentrations of AgNP, FA and Na_2S were 1,000 mg L^{-1}, 5,000 mg L^{-1}, and 6.5 mM, respectively, where FA (eq) represents samples that allowed equilibration of FA and AgNP to equilibrate prior to sulfide addition. The dashed lines show least square fitting using first order kinetic law. The error bars of Na_2S control represent standard deviation of triplicate experiments. Other data were measured in one batch. (B) Sulfide depletion as a function of NOM component property in the absence of

AgNPs (break in *x* axis represent duration from 250 min to 400 min). The freshly prepared and pH adjusted FA and HA stock solutions were aged in glass vials protected from the light for 12 months and 18 months, respectively. The concentrations of NOM and Na_2S were 5,000 mg L^{-1} and 6.5 mM, respectively. Data reports percent sulfide concentration normalized to the initial sulfide in MHRW. The data represent σ for $n > 5$ measurements from the same stock aged for different durations.

The competing processes (e.g., sulfidation of AgNPs, sulfide interaction with FA, oxidation of sulfide, etc.) convoluting individual rate interpretation demonstrate the inability of the direct ISE method alone to discriminate sulfidation of AgNP. The results in Figure 1 also indicated that NOM components are a sink for measurable sulfide species. The sulfidation potential of the solution containing multiple S-containing species (e.g., sulfide-FA adduct, free sulfide species, and elemental sulfur) may result in disparate reaction pathways (i.e., rates) for AgNP sulfidation in the environment, which has not been explicitly reported in the literature.

To examine whether measuring free sulfide could reveal information regarding sulfide potential in suspensions where large free sulfide sinks exist, we first varied the NOM component type (FA and HA) and chemical state (aging) to investigate their contribution to observed sulfidation consumption. Here, aging represents the time in which a resuspended NOM component was stored in darkness. Rapid decrease in sulfide concentration was observed in all conditions, but sulfide reacted relatively slower with HA than FA (Fig. 1B). Additionally, aging of dissolved NOM components appeared to play a role. Overall, although disparate rates for pristine FA and HA were observed, aged NOM components started to exhibit converging rates, which may affect both AgNP corrosion and coverage (Fig. 1B and S1). Possible pathways and products of sulfide-NOM reactions include: (1) oxidation of sulfide to higher oxidation states (S^0 and $S_2O_3^{2-}$) by reduced quinone moieties in NOM, (2) incorporation of S into NOM structure to organic sulfur compounds (i.e., thiols, di- and polysulfides, or heterocycles),[18, 19] and (3) adsorption of H_2S onto non-polar groups,[8] We demonstrate the source of the sulfide would affect the sulfidation and associated rates of AgNP, but identifying the nature and chemical structure of the sulfide source and contribution of NOM aging was outside the current scope.

Although the direct method could not distinguish sulfidation of AgNP from NOM components, ISE measurements were conducted via an analyte subtraction method, which estimates sulfide availability by stoichiometric consumption of Ag^+ and were compared to the direct method in the absence of AgNP (see ESI for further details). The analyte subtraction and direct calibration methods reproducibly measured sulfide in the absence of NOM components (Fig. 2, square symbols), where error bars represent σ for $n \geq 5$. In the presence of FA, the analyte subtraction approach consistently resulted in higher sulfide concentrations probably due to improved sensitivity for active sulfur species other than $H_{2-n}S^{n-2}$ (Fig. 2, triangle symbols). To examine whether the sulfide-FA adducts are the primary contribution to the concentration gap, we used centrifugal ultrafiltration (Amicon Ultra-4, nominal molecular weight limit of 3 kDa) to remove the FA. The sulfide in FA-free filtrates were comparable with $H_{2-n}S^{n-2}$ in unfiltered mixture (measured via direct calibration approach), but were significantly lower than the total active sulfur compounds (measured by analyte subtraction approach) (Fig. S2). The concentration difference represented sulfur-containing species that are active for the sulfidation reaction but are undetected by direct calibration approach. Because the ISE measurement underestimated this population by the direct calibration approach, the calculated kinetic rates for AgNP sulfidation will be overestimated (Fig. 1).

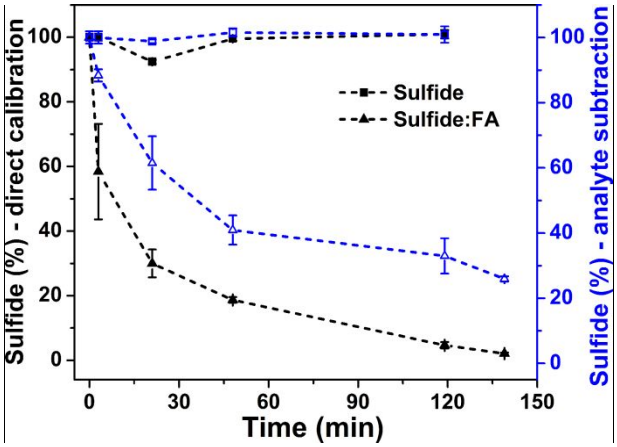

Figure 2. Comparison of sulfide ISE measurement via the direct calibration (black) and analyte subtraction approach (blue) in Na_2S solution (square symbol) and Na_2S/FA mixture (triangle symbol). The concentrations of Na_2S and FA were 4.5 mM, and 3,500 mg L^{-1}, respectively. Data are normalized to concentration measured at t = 0 min in Na_2S solution and show average and standard deviation of duplicate experiments.

After demonstrating the analyte subtraction method was more sensitive than the direct approach for monitoring available sulfide species in the absence of AgNP, we used analyte subtraction to examine the sulfide depletion kinetics in the presence of AgNP. Two concentrations of AgNP were used for comparison to the *in situ* XRD measurements (1400 mg mL^{-1}, Figure 3A) and near the detection limits for the ISE measurements (150 mg mL^{-1}, Figure 3B). First, we observed faster sulfide consumption in FA (Na_2S:FA), AgNP alone ([S]/[Ag]) and FA:AgNP ([S]/[Ag]=0.7:FA) systems than the solution phase oxidation of Na_2S (Fig. 3A). Under FA free conditions, AgNP sulfidation follows a two-stage reaction with transition point near ≈ 3 h, which was consistent with previous reports for fast and slow consumption of sulfide and attributed to AgNP sulfidation and aqueous phase oxidation (dissolved oxygen), respectively.[14] To compare data to previous studies, a two-stage first order kinetic law was used:

$$-dC_t / dt = (k_{Ag} + k_{homogen}) \times C_t \qquad \text{Eq. 1}$$

where C_t is the sulfide concentration at time t, k_{Ag} and $k_{homogen}$ are the rate constants of sulfidation and homogeneous oxidation processes, respectively, giving k_{Ag} (0 - 5 h) = 0.006 ± 0.01 min^{-1} and $k_{homogen}$ = 0.001 ± 0.001 min^{-1}. The observed k_{Ag} is an order of magnitude lower than that for uncoated 30 nm AgNPs,[14] where the decrease in rate could be partly attributed to the decrease in surface area (approximately 5x difference) and possibly crystallinity.[13,14] Considering the preservation of PVP on sulfidized AgNP surfaces an additional contribution from surface attached PVP is also possible.[24] Faster sulfide depletion was observed in [S]/[Ag]=0.7:FA at 1400 mg mL^{-1} (green, hollow triangle) than for AgNPs sulfidation (red circles), but the kinetics are nearly identical to Na_2S:FA control (blue triangles) at the higher AgNP concentration (Fig 3A). A steady state following the initial rapid concentration drop after approximately 2 h was observed. An equilibrium constant was necessary to fit the first-order kinetic law:

$$-d(C_t - C_{eq}) / dt = k_{obs} \times (C_t - C_{eq}) \qquad \text{Eq-2}$$

where C_{eq} is the equilibrium concentration at the later stage of reaction. For [S]/[Ag]=0.7:FA sulfidation and Na_2S:FA control samples, k_{obs} of (0.027 ± 0.001) min^{-1} and (0.031 ± 0.001) min^{-1}, and C_{eq} / C_0 of 10% and 13% were obtained respectively. The requirement of the C_{eq} value suggests that NOM components

preserve sulfidation potential in the solution and illustrate clear differences in Ag sulfidation in the presence and absence of NOM components. Furthermore, differences between measured sulfidation with the two NOM components was also observed. The C_{eq} / C is substantially lower in AgNP-HA systems (21%) than in Na_2S/HA control sample (34%), indicating sulfide consumption was enhanced in the presence of AgNPs. In addition, AgNP equilibrated with FA prior to sulfide addition showed no effect on sulfide depletion rate (Fig. S3), and the aged FA resulted in slower reaction with Na_2S (Fig. S4). In general, compared with ISE results using direct calibration approach, the rates determined using analyte subtraction approach were slower due to improved sensitivity towards active organic sulfur species, but the rate for AgNP sulfidation still cannot be easily deconvoluted in the systems containing NOM.

Differences in sulfidation kinetics were observed at lower concentrations of AgNPs (150 mg L^{-1}, m_{FA}/m_{Ag} = 5)). As shown in Fig. 3B, data fitting using Eq-2 gives rate constants on the order of AgNPs/FA sulfidation > Na_2S/FA control > AgNPs sulfidation, where k_{obs} are (0.020 ± 0.002) min^{-1}, (0.010 ± 0.002) min^{-1}, and (0.007 ± 0.0003) min^{-1}, respectively. The results at lower concentrations, where Na_2S reacts with FA and AgNPs at similar rates, demonstrate the additive effect of NOM induced sulfide consumption on the apparent rate of AgNP sulfidation in the presence of FA. However, deconvoluting the combined process and distinguishing reaction rates for AgNP sulfidation remains intractable with ISE alone.

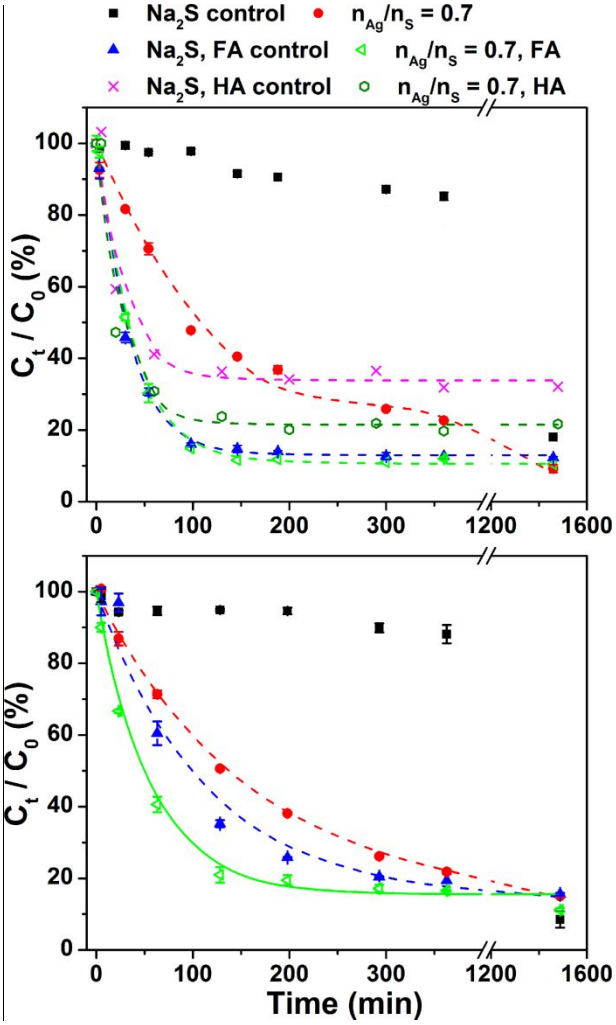

Figure 3. Time-resolved sulfide measurements by ISE *via* the analyte subtraction approach for AgNP sulfidation at AgNP concentration of (A) 1400 mg mL^{-1}, and (B) 150 mg mL^{-1}. The concentrations of AgNP, FA (HA) and Na_2S in (A) were 1,400 mg L^{-1}, 7,000 mg L^{-1}, and 9.1 mM, respectively. The concentrations of AgNP, FA and Na_2S in (B) were 150 mg L^{-1}, 750 mg L^{-1}, and 1.0 mM, respectively. The dashed lines show least square fitting using first order kinetic law and error bars represent standard deviation of replicate experiments (n≥2). The breaks in *x*-axis represent duration from 400 min to 1200 min.

AgNP sulfidation examined by in-situ XRD

Although the analyte subtraction method with ISE provides better sensitivity for S-containing species, the question remains whether the observed sulfide consumption directly relates to Ag^0 conversion. To examine the mechanisms governing corrosion (oxidation and sulfidation) on the AgNP surface and whether they can be examined with proxy measurements, direct measurements of NP composition are necessary. Coupling the composition measurements with the previously quantified ligand coverage data[25] provides a more complete understanding regarding specific contributions to NP corrosion in natural and engineered systems. Similar experiments at 1,600 mg L^{-1} of PVP-AgNP, and the effect of NOM components and pH were examined by *in situ* synchrotron XRD and *ex situ* TEM.

For all the PVP-AgNP systems, diffraction peaks emerging with the concomitant decrease in Ag (220) peak were assigned to Ag_2S (acanthite) and supported direct transformation of Ag^0 to Ag_2S.[20] Results of time resolved intensity change for Ag^0 characteristic peak are summarized in Figure 4, where pseudo first order fits used for ISE were used for direct comparison between measurement methods. In the PVP-AgNP only ([S]/[Ag]), a multiple stage decay of Ag^0 (transformation) was observed, where an initial relatively slow rate of decay was observed until ≈130 min and was proceeded by a faster decay until an asymptote was reached near 80 % conversion of Ag^0. The corresponding rate constants from a pseudo first order exponential decay were (0.004 ± 0.001) min^{-1} and (0.013 ± 0.001) min^{-1}, respectively. The rate model was only used to compare the current and previously reported sulfidation rates from proxy measurements. The reaction rate becomes essentially null in < 250 min. The increased rate of conversion represents a change in the mechanism for Ag^0 corrosion that was not observed in ISE. In the presence of FA and HA, the reaction rates were nearly identical (0.014 ± 0.001) within the uncertainty of the fit. However, the percent conversion after 300 min in the presence of HA (≈63%) was greater than in the presence of FA (≈55%). Overall, the rates observed were different than observed with ISE, and in some cases almost an order of magnitude different. Additionally, for all samples examined, the time length for observed Ag^0 decay were different than the time periods observed for sulfide decay.

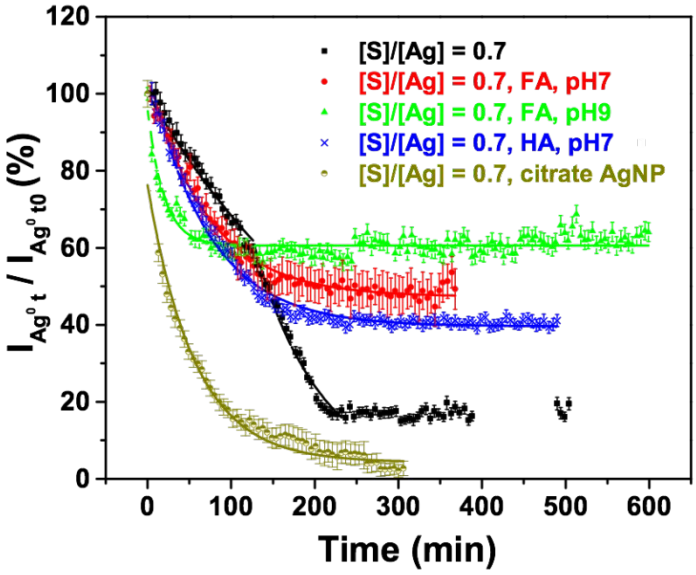

Figure 4. Time-resolved evolution of integrated Ag peak intensity upon addition of Na_2S. The concentrations of AgNP, FA (HA) and Na_2S in were 1,600 mg L^{-1}, 8,000 mg L^{-1}, and 10.4 mM, respectively. Under all testing conditions, sulfidation processes were directly evident from the decrease of diffraction peak intensities associated with Ag^0 and the appearance of diffraction peaks consistent with Ag_2S (acanthite).

In an initial effort to distinguish the contributions from engineered coatings and the currently employed NOM components, additional *in situ* XRD experiments were conducted with commercially available citrate coated NPs. In citrate-coated AgNP systems in the absence of FA, disparate processing was observed from PVP-coated samples (Figure 4). First, a single exponential decay of Ag^0 was observed over 300 min for the citrate sample ([S]/[Ag]=0.7 citrate-AgNP, gold trace), which was faster than any other system at pH 7 examined (Table 1). Second, the extent of Ag to Ag_2S conversion was nearly complete over the same time period based on diffraction, which was higher than any other system observed. The resulting sulfidated products from the citrate coated AgNPs were shown to be porous with TEM (Fig. S5). However, these results are distinct from previous reports on total conversion, which may be a resulting from different AgNP properties (size), sample preparation, or sensitivity of measurements used. This is also in contrast to previous work by the author, which predicted nearly saturated levels of dissolved oxygen in all solutions at these concentrations would result in complete conversion.[3] However, complete conversion of all 70 nm AgNP was observed near [S]/[Ag] ≥ 1.

The hypothesis that the observed quenching of the reaction occurs when the initial Ag^0 available for oxidation is consumed, i.e., the formation of Ag_2S shell on the NP surface was a barrier for reaction, was also consistent with the rate of conversion observed in the PVP-AgNP samples at pH 9. AgNP sulfidation in the presence of FA (green trace, Fig. 4) exhibited the fastest initial rate for PVP-AgNP, but the total conversion was below all pH 7 systems. The sulfidation was essentially quenched in < 120 min. The overall reaction for oxysulfidation at pH 9 includes first oxidation of Ag^0 to Ag^+ to form Ag_2S through:

$$4Ag + O_2 + 2HS^- \rightarrow 2Ag_2S + 2OH^-$$

Increasing the pH from 7 to 9 increases the concentration of HS^- (pKa of $H_2S \approx 7$), but the oxidation potential of the solution is decreased and could inhibit Ag_2S formation through a slower oxidation rate. The

increase in pH also affects the solubility of the metal complexes and Ag_2S products. The faster quenching and lower conversion of Ag^0 observed in the diffraction data suggests either i) the relative rate of Ag oxidation was too slow to continue to promote Ag_2S formation, even in systems stirred in ambient conditions (nearly constant dissolved oxygen concentration), ii) the formation of a nearly continuous coating (i.e., crystalline) of Ag_2S was present resulting in a (nearly) null reaction rate, or iii) a combination of multiple processes including i) and ii) which affects the nucleation and growth of Ag_2S. Overall, clear differences in the presence of PVP, introduction of NOM constituents, and amount of SH^- all play a role in the rate and extent of processing that occurs during AgNP sulfidation. Although the global rates of sulfidation where within an order of magnitude using ISE, differentiating the loss of sulfide through reactions with the organic material and the conversion of Ag to Ag_2S could not be accomplished without XRD and TEM.

Implications for improved understanding of AgNP sulfidation mechanisms

To assemble a more complete mechanistic picture for AgNP sulfidation in aqueous systems, the relationship between sulfide consumption, AgNP sulfidation and surface chemical changes must be considered. First, in [S]/[Ag]=0.7 samples, comparison of the sulfide consumption and Ag^0 consumption were the simplest to compare because no complications from NOM components were present. The consumption of sulfide persisted throughout the experiment, where k_{Ag} in (0 - 5 h) with ISE was (0.006 ± 0.001) min^{-1}. Although the rates were reported to be similar using an C_{eq}, if the contribution from oxidation was subtracted, the calculated rate without C_{eq} was (0.013 ± 0.002) min^{-1}. The sulfidation rate was similar to the secondary catalyzed rate that was observed after 130 min with XRD. However, no salient feature for a transition from one regime to another could be identified from the ISE results, indicating an insensitivity to changes in sulfidation processes. ISE measurements also exhibited continuous decay for the systems that did not contain NOM components. The unchanging peak intensities observed in the XRD data at t = 230 min while sulfide consumption was observed, provided the clearest evidence for difficulties with correlating sulfide consumption and silver sulfidation with only ISE measurements.

The sulfidation of AgNPs in the presence of NOM components resulted in similar rates at pH 7. However, two clear differences have been reported between HA and FA in the current system and provide insight into their contribution on chemical and structural changes during AgNP sulfidation. First, the amount of FA adsorbed to the AgNP surface was more than three times greater than in the HA system.[25] Second, the interaction of free sulfide with freshly prepared HA was slower than systems with freshly prepared FA (Fig. 1). These differences can be attributed to specific contributions from the NOM components. The former suggests that NOM coverage contributes to the relative extent of processing that occurs before the initial sulfidation rate decays to nearly undetectable changes of Ag^0 (i.e., essentially a null reaction based on minute to hour time scales observed for the *in situ* experiments). Because the measured AgNP sulfidation rates are essentially equivalent for the FA and HA systems, the latter suggests the rate seemingly is not dependent on the concentration of free sulfide in solution.

Together, the first direct relationship between total coverage (engineered coating and NOM components) on Ag^0NP and Ag_2S formation clearly emerged. Changes in the total sulfide consumption were lower in HA:AgNP system than FA:AgNP the systems (Fig. 3A), even though the conversion of Ag to Ag_2S observed was higher for HA system. This fact directly demonstrates total consumption of sulfide was not an indicator of Ag corrosion, and the competing rates of consumption of sulfide with the NOM components

and oxidation must be incorporated (i.e., the rate expression must not be zero order with respect to either adsorbed or total organic materials in the systems.) The ISE data also showed conservation of sulfide in the presence of HA after initial consumption (< 200 min), which did not occur in [S]/[Ag]=0.7, and suggests the NOM components may preserve sulfidation potential in the solution for more than 24 h. In comparison to previous work on citrate-AgNP that suggested adsorbed HA facilitated sulfide to surface,[8] HA did slightly increase the rate of sulfidation compared to [S]/[Ag]=0.7. However, the increased rate may be induced by HA preserving sulfidation potential in the solution rather than the previously hypothesized role of adsorbed species. The preservation of sulfidation potential in the presence of NOM components may also cause differences in samples examined with *ex situ* measurements (e.g., X-ray absorption methods), but work to investigate possible measurement artifacts was beyond the current scope.

Although previous work has suggested the PVP-coating contributes to mass preservation, direct comparison of PVP-AgNP to citrate-coated AgNPs allowed separating the contribution of engineered coatings from NOM components on the observed sulfidation rate and subsequently, structural changes.[20] The porous structures resulting from citrate-coated AgNP sulfidation were never detected in PVP-AgNP samples examined with SAXS/USAXS. SAXS measurements statistically sample the NP population in suspensions and are highly sensitive probes to changes in NP volume and structure, which can readily detect the porous structures observed in TEM. The formation of voids during sulfidation of citrate coated AgNPs in the presence of HA was also previously reported.[8] Therefore, we surmise HA does not promote the formation of the porous structures as suggested. Instead, the structural changes are likely due to lower coverages on the AgNP surface, where HA has a lower affinity to the AgNP surface relative to FA along with the absence of PVP, promoting faster Ag^0 to Ag_2S conversion and porous structures. The mechanism for conversion represents the faster diffusion of silver to the NP surface, possibly via the Kirkendall effect, to create the observed voids as reported previously.[8] Ongoing work is focused on better understanding the relationship between observed structural changes and ligand shell components (i.e., electronic surface structure) in metallic nanoparticles during corrosion.

Direct contributions from both the engineered coating and NOM component were isolated. Overall, an inverse relationship between coverage and conversion was observed. A summary of the findings from the current system are found in Figure 5. Understanding the contributions from molecular species on the NP surface during transformations continues to be an active area of research, which likely will require a combination of ensemble and single nanoparticle methods. Because reported dissolution of Ag ions from partially sulfidated AgNPs was different based on the source of the FA[26] and changing suspension stabilities have also been reported for different NOM component sources,[27] further work on quantifying heterogeneous coatings on the NPs with different engineered coatings and their contributions to the extent of transformation are warranted. For more complex systems, competing reactions with more disparate rates are likely to be observed, such as in systems where dissolution of Ag_2S are known to occur.[28] The current work demonstrates the limitations of ISE measurements, but also clearly identifies the need for quantifying and understanding the role of engineered and heterogeneous coatings on metallic NPs transformation pathways to improve performance and stability of current and emerging metallic NP-based technologies. To understand the mechanistic details of metallic NP transformations for improved performance and design in applied systems, the measurement methods employed must be sensitive to the reaction of interest, which we demonstrate is not the case for ISE or generally other indirect measurements, and include thorough surface characterization when coatings are present.

Table 1. Summary of AgNP sulfidation kinetics measured by both ISE_{Direct}, $ISE_{Anal-Sub}$, and *in situ* XRD in MHRW containing [S]/[Ag] = 0.7.

Sample	K_{obs} (min^{-1}) (ISE_{Direct})	K_{obs} (min^{-1}) ($ISE_{Anal-Sub}$)	K_{obs} (min^{-1}) (XRD)	Ag^0 conversion (%, XRD)
Na_2S + FA; pH 7 *No NPs*	(0.096 ± 0.002)	(0.010 ± 0.002)	--	--
PVP-AgNP				
[S]/[Ag] = 0.7, pH7	--	(0.007 ± 0.0003)	(0.004 ± 0.001) (0.013 ± 0.001)	83
[S]/[Ag] = 0.7, FA, pH 7	(0.099 ± 0.008)	(0.020 ± 0.002)	(0.014 ± 0.001)	55
[S]/[Ag] = 0.7, FA, pH 9	--	--	(0.051 ± 0.005)	36
[S]/[Ag] = 0.7, HA, pH 7	--	--	(0.014 ± 0.001)	63
Citrate-AgNP				
[S]/[Ag] = 0.7, pH 7	--	--	(0.21 ± 0.005)	98

*ISE_{Direct} represents the direct method, $ISE_{Anal-Sub}$ represents the analyte subtraction method and XRD represents the synchrotron-based *in situ* method. For XRD measurements using WAXS, Ag^0 conversion percent represents the quantified area loss of the Ag (220) peak. TEM results qualitatively supported the findings on conversion measured from XRD.

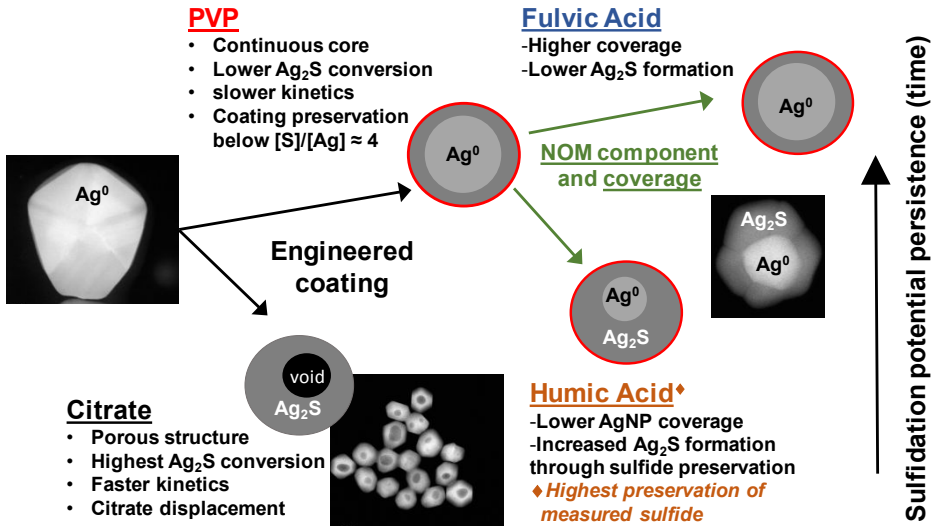

Figure 5. Summary of proposed contributions from engineered coatings, media components and sulfide preservation on the measured rate of AgNP sulfidation elucidated using ISE and *in situ* XRD measurements. Sulfidation potential persistence here referred to the amount of time after sulfide addition the ISE analytical subtraction method could detect available sulfide, where the interaction of HS^- and H_2S with the NOM components results in measurable sulfide preservation. TEM images for citrate demonstrate the porous structure observed in contrast to the preserved

Ag^0 core and lobed growth observed in PVP-AgNP systems (red outline demonstrates PVP persistence on AgNP surface). Higher conversion of Ag to Ag_2S was *inversely proportional* to ligand coverage for all systems.

Conclusions

The current work investigated the use of ISE methods to follow corrosion of AgNPs in aqueous media, which contained environmental constituents, and specifically, components of NOM. A direct relationship between sulfide consumption and Ag to Ag_2S conversion could not be elucidated, because the sulfide consumption was nonuniform in the presence of different NOM components and engineered coatings. The *in situ* XRD data revealed distinct processing based on engineered and NOM coatings. Although the rates of the sulfidation were similar (within the same order of magnitude) to previous reports using XRD, distinct reaction regimes could be identified, e.g., PVP-AgNP, that were indistinguishable in ISE measurements and the goodness of fits for pseudo first order decay varied, indicating changing reaction mechanisms. Measured sulfide consumption also did not occur on the same time scales as Ag corrosion due to competing reactions of sulfide with NOM and AgNPs. The role of organic molecules (engineered or present in system) on the surface affected the measured sulfidation rate and more prominently the extent of transformation, which suggests Ag to Ag_2S transformations are affected by both the concentration of sulfide present and the interfacial properties of the NP. The presence of incomplete and nonuniform processing observed on the NP surface changes their intrinsic optical, electronic and catalytic properties, and therefore, their performance and fate.

For AgNP sulfidation, the role of the organic molecules has only been previously suggested to affect the rate of transformations occurring in similar AgNP systems, but no direct measurements have been presented to investigate individual contributions. By combining the current work with *in situ* surface chemical characterization and structural investigations, the factors contributing to each product population can begin to be attributed to their corresponding transformation pathways with relative rate expressions in each identified reaction regime, which is currently ongoing work. Overall, the current study provided evidence that direct measurements are needed to determine the influencing factors of adsorbed NOM components, engineered coatings and rate of sulfidation on the formation mechanism of Ag_2S in simulated media. Although NOM components are used for the organic coatings to affect Ag_2S formation, the current measurement methods examined should also facilitate better design of metal-semiconductor hybrid systems that have shown promise for catalysis, photonics and sensing applications.

Acknowledgement

Use of the Advanced Photon Source, an Office of Science User Facility operated for the U.S. Department of Energy (DOE) Office of Science by Argonne National Laboratory, was supported by the U.S. DOE under Contract No. DE-AC02-06CH11357.

References

1. U. Banin, Y. Ben-Shahar and K. Vinokurov, *Chemistry of Materials*, 2014, **26**, 97-110.
2. H. Song, *Accounts of Chemical Research*, 2015, **48**, 491-499.
3. T. Li, A. J. Senesi and B. Lee, *Chemical reviews*, 2016, **116**, 11128-11180.
4. Y. Sun, X. Zuo, S. K. Sankaranarayanan, S. Peng, B. Narayanan and G. Kamath, *Science*, 2017, **356**, 303-307.
5. J. Liu, Z. Wang, F. D. Liu, A. B. Kane and R. H. Hurt, *ACS nano*, 2012, **6**, 9887-9899.
6. J. Liu, K. G. Pennell and R. H. Hurt, *Environmental science & technology*, 2011, **45**, 7345-7353.

7. C. Levard, B. C. Reinsch, F. M. Michel, C. Oumahi, G. V. Lowry and G. E. Brown Jr, *Environmental science & technology*, 2011, **45**, 5260-5266.
8. B. Thalmann, A. Voegelin, E. Morgenroth and R. Kaegi, *Environmental Science: Nano*, 2016, **3**, 203-212.
9. W. Zhang, B. Xiao and T. Fang, *Chemosphere*, 2018, **191**, 324-334.
10. J. Y. Liu, K. G. Pennell and R. H. Hurt, *Environmental Science & Technology*, 2011, **45**, 7345-7353.
11. Y. Q. Zhang, J. C. Xia, Y. L. Liu, L. W. Qjang and L. Y. Zhu, *Environmental science & technology*, 2016, **50**, 13283-13290.
12. C. Levard, B. C. Reinsch, F. M. Michel, C. Oumahi, G. V. Lowry and G. E. Brown, *Environ. Sci. Technol.*, 2011, **45**, 5260-5266.
13. B. Thalmann, A. Voegelin, E. Morgenroth and R. Kaegi, *Environ-Sci Nano*, 2016, **3**, 203-212.
14. R. Ma, J. Stegemeier, C. Levard, J. G. Dale, C. W. Noack, T. Yang, G. E. Brown and G. V. Lowry, *Environ-Sci Nano*, 2014, **1**, 347-357.
15. R. Ma, C. Levard, F. M. Michel, G. E. Brown and G. V. Lowry, *Environmental science & technology*, 2013, **47**, 2527-2534.
16. *Report of Investigation for Reference Material 8017, Polyvinylpyrrolidone Coated Silver Nanoparticles, Nominal Diameter 75 nm*, National Institute of Standards and Technology, Gaithersburg, MD, 2015.
17. *Journal*, 2002.
18. Z. G. Yu, S. Peiffer, J. Gottlicher and K. H. Knorr, *Environmental science & technology*, 2015, **49**, 5441-5449.
19. T. Heitmann and C. Blodau, *Chem Geol*, 2006, **235**, 12-20.
20. F. Zhang, A. J. Allen, A. C. Johnston-Peck, J. Liu and J. M. Pettibone, *Nanoscale Advances*, 2018, DOI: 10.1039/C8NA00103K.
21. G. Dimeski, T. Badrick and A. S. John, *Clinica Chimica Acta*, 2010, **411**, 309-317.
22. E. Bakker, E. Pretsch and P. Bühlmann, *Analytical Chemistry*, 2000, **72**, 1127-1133.
23. K. Y. Chen and J. C. Morris, *Environmental Science & Technology*, 1972, **6**, 529-537.
24. J. M. Pettibone and J. Y. Liu, *Environmental science & technology*, 2016, **50**, 11145-11153.
25. J. M. Pettibone, J. M. Gorhman and J. Liu, *Journal of Nanoparticle Research*, 2018, DOI: 10.1007/s11051-018-4410-4.
26. B. Collin, O. V. Tsyusko, D. L. Starnes and J. M. Unrine, *Environmental Science: Nano*, 2016, **3**, 728-736.
27. I. L. Gunsolus, M. P. S. Mousavi, K. Hussein, P. Bühlmann and C. L. Haynes, *Environmental Science & Technology*, 2015, DOI: 10.1021/acs.est.5b01496.
28. L. Li, Q. Zhou, F. Geng, Y. Wang and G. Jiang, *Environmental Science & Technology*, 2016, **50**, 13342-13350.

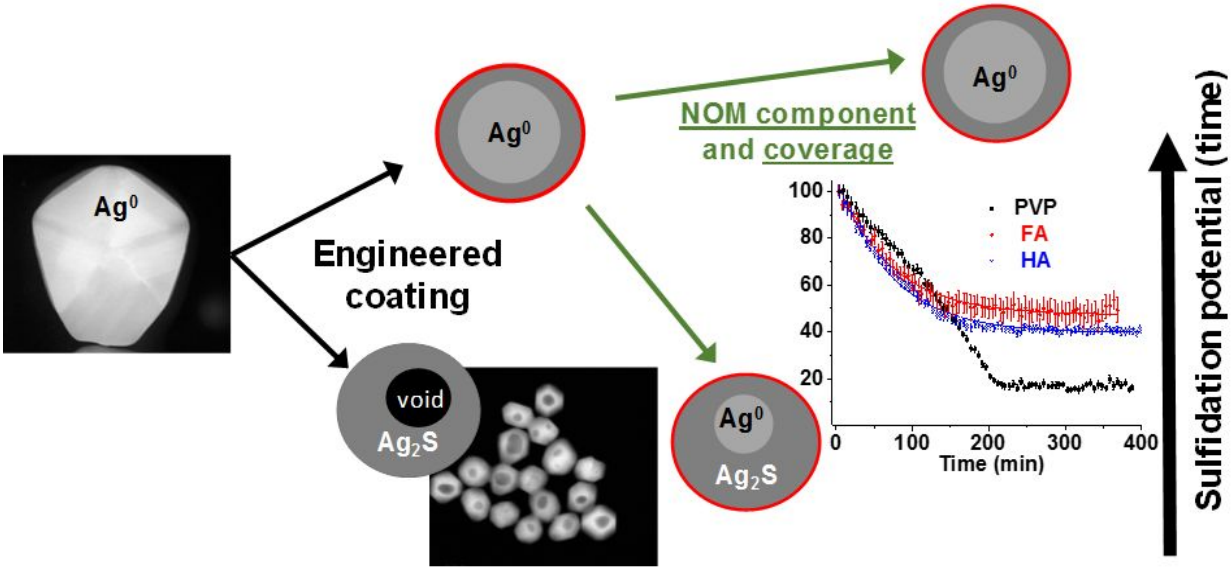
Ag0
Engineered coating
Ag0
void
Ag2S
Ag0
NOM component and coverage
Ag0
Ag2S
100
80
60
40
20
0
100
200
300
400
Time (min)
PVP
FA
HA
Sulfidation potential (time)